Ecological Indicators 150 (2023) 110232

Contents lists available at ScienceDirect

Ecological Indicators

journal homepage: www.elsevier.com/locate/ecolind

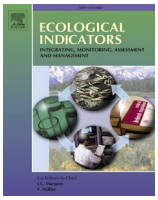

Modelling time-series *Aedes albopictus* abundance as a forecasting tool in urban environments

Alessandra Torina [a,1], Francesco La Russa [a,1], Valeria Blanda [a,*], Alfonso Peralbo-Moreno [b], Laia Casades-Martí [b], Liliana Di Pasquale [a], Carmelo Bongiorno [a], Valeria Vitale Badaco [a], Luciano Toma [c], Francisco Ruiz-Fons [b,d]

[a] *Istituto Zooprofilattico Sperimentale della Sicilia "A.Mirri", Palermo, Italy*
[b] *Instituto de Investigación en Recursos Cinegéticos (IREC), CSIC-UCLM-JCCM. Ronda de Toledo, Ciudad Real 12. 13005, Spain*
[c] *Dipartimento Malattie Infettive, Reparto Malattie Trasmesse da Vettori, Istituto Superiore di Sanità, Rome 00161, Italy*
[d] *CIBERINFEC (ISCIII), CIBER de Enfermedades Infecciosas, Instituto de Salud Carlos III, Madrid 28029, Spain*

ARTICLE INFO

Keywords:
Invasive species
Meteorological modelling
Mosquito
Population dynamics
Vector-borne disease

ABSTRACT

Aedes albopictus is an invasive mosquito species that can maintain and transmit several arboviruses causing disease in humans. Understanding the determinants of its ecology and population dynamics to predict its abundance was the main objective of this study.

Adult mosquitoes were captured weekly between 2009 and 2016 with BG sentinel traps baited with BG-Lure outdoors at a collection site within the urban area of Palermo (southern Italy). In parallel, between 2012 and 2016, we monitored the uninterrupted weekly abundance of *Ae. albopictus* at four additional sites nearby over an area of about two hectares. Catches were collected three times per week and mosquitoes were identified morphologically.

To identify the determinants of mosquito abundance, seasonal autoregressive integrated moving-average and Poisson regression models were fitted to the weekly abundance of *Ae. albopictus* with a series of weather predictors that potentially modulate its activity and population dynamics. The time lag of the influence of predictors was analysed to identify the intergenerational environmental determinants of *Ae. albopictus* population dynamics. A cross-validation of the predictive accuracy of the different models was carried out to select the best predictive model.

Over 7 years we captured 12,152 *Ae. albopictus* in the first trap and another 58,710 in four years of trapping in four additional traps. *Aedes albopictus* abundance was highly seasonal, with activity between mid-March and late December, highest abundances between July and September, and peak abundances in autumn. The predictive potential of the best model was further externally validated with four years of data from the other four traps, showing a high predictive capacity and a very good fit of seasonality and abundance peaks. Relative humidity, vapour saturation deficit and wind speed were identified as the main determinants of the weekly abundance of *Ae. albopictus*. The results obtained will allow accurate prediction of the abundance of this invasive mosquito in coastal Mediterranean areas and the design of ad-hoc measures for efficient and environmentally sustainable control.

1. Introduction

Mosquitoes (Order Diptera, Family Culicidae) are cosmopolitan hematophagous insects with a great capacity to adapt to changing environmental conditions, in part due to their great global diversity with more than 3,000 species. Many mosquito species are of great health concern and represent a serious nuisance to humans. Among them, *Aedes albopictus* is an outdoor, diurnal mosquito that feeds preferentially on humans and is classified as an invasive species outside its original tropical range in Asia and Oceania due to its high ecological plasticity (i.

* Corresponding author.
E-mail address: valeria.blanda@izssicilia.it (V. Blanda).
[1] Equal contribution.

https://doi.org/10.1016/j.ecolind.2023.110232
Received 8 August 2022; Received in revised form 9 March 2023; Accepted 6 April 2023
Available online 8 April 2023

Fig. 1. Spatial location of the trapping sites at Istituto Zooprofilattico Sperimentale of Sicily, Palermo and detailed view of the BG Sentinel traps placed at trapping sites 1 to 5 as described in the text.

e., colonises both artificial and natural breeding sites) and physiological characteristics (i.e., eggs highly resistant to desiccation and freezing), which allow the species to spread and establish successfully in both tropical and temperate regions (Mercier et al., 2022). *Aedes albopictus* is one of the invasive mosquito species that have recently become established in Europe (ECDC & EFSA, 2021) and it is one of the 100 World's Worst Invasive Allien Species identified by the IUCN (https://www.iucngisd.org/gisd/). Its colonisation has become a public health problem not only because of the nuisance due to its aggressive outdoor diurnal biting behaviour, but especially because it is a competent vector of many human viruses, such as Dengue virus, Chikungunya virus, Zika virus and Usutu virus (Johnson et al., 2018). This invasive mosquito species has already colonized numerous European countries, which implies a serious risk that the timely introduction of the pathogens it transmits could lead to them becoming endemic. In Italy, *Ae. albopictus* was introduced in September 1990 in Genoa (Sabatini et al., 1990) from where the species has colonised the entire country (ECDC & EFSA, 2021). In 2007, the abundant and well-established *Ae. albopictus* population in the region of Emilia Romagna (north-eastern Italy) was responsible of the first autochthonous outbreak of chikungunya in Europe, after the virus was presumably introduced into an infected patient from India (Rezza et al., 2007). The presence of *Ae. albopictus* was first documented in Palermo (Sicily, southern Italy) in the autumn of 2004 and in 2005 the first monitoring was carried out at 28 sites with 300 ovitraps (Torina et al., 2006). On these premises, an effective control strategy is essential to reduce *Ae. albopictus* biting rates and pathogen transmission potential in colonised areas. Different control methods (environmental, mechanical, biological, chemical, and genetic) have been proposed and used as a part of an integrated control strategy for invasive mosquito species in different European countries with varying effectiveness (Baldacchino et al., 2015; Macaluso et al., 2021). Effective control interventions in areas permanently colonized by a mosquito species require a prior identification of the spatial and temporal hotspots of mosquito abundance. Therefore, understanding vector population dynamics in relation to ecological drivers is essential to assess the implementation of cost-effective and more environmentally friendly control strategies.

Transmission of mosquito-borne pathogens is strongly related to vector abundance (Kilpatrick and Pape, 2013) and mosquito population dynamics shape pathogen transmission dynamics. Therefore, being able to predict vector abundance patterns in advance can lead to better forecasting pathogen transmission probabilities to effectively control vectors and prevent health risks (Cuadrado-Matías et al., 2022). However, the generation of predictive models with robust forecasting capacity requires accurate information on vector dynamics obtained from long time series reliable enough to inform with precision on important

aspects such as seasonality, population trend or the stochastic occurrence of abundance peaks (Lebl et al., 2013; Groen et al., 2017). This information is only available through entomological monitoring programmes over long time series and, in general, the information available is often limited either spatially or temporally. Most studies on mosquito distribution and abundance tend to be conducted at large spatial scales and with temporal limitations (Durán-Martínez, 2012), and even when conducted at lower spatial scales, they usually cover a short time monitoring period (Cianci et al., 2015). Different approaches can be helpful to identify the main determinants of mosquito seasonality, dynamics and focal abundance and thus predict population dynamics. Autoregressive (AR) integrated (I) moving-average (MA) models (ARIMA) would be practical in forecasting weekly *Ae. albopictus* captures for a specific time based upon previous capture numbers, the random variation of past captures and a given level of integration. The order of an ARIMA model is indicated by 'p', 'd' and 'q' values within brackets (p, d, q). Seasonal ARIMA (SARIMA) models allow including seasonal effects (s) observed in time series data (P, D, Q, s). Seasonality is inherent to arthropod vectors' activity patterns in temperate areas of the Earth (e.g., Geoghegan et al., 2014). Poisson regression also allows building accurate predictive models on time series count data (see Walsh et al., 2008; Lebl et al., 2013). However, linear regression may be seriously affected by common statistical problems arising from the nature of the covariates, their relationships, the presence of outliers or the presence of variation differences (Zuur et al., 2010). If the aim of the regression is answering major questions underlying an ecological system and inferring causal associations for natural phenomena, particular aspects of the covariates and their relationships may alter model coefficients, resulting in the erroneous interpretation of covariate effects.

The present study aimed to investigate over an extended period of time the seasonal abundance and dynamics of adult *Ae. albopictus* mosquitoes in a restricted urban area of Palermo (Sicily) where this invasive species is already well established. The study also aimed to fit predictive models to time series data on *Ae. albopictus* counts to weather quantities to understand the abiotic factors driving its population dynamics and to accurately predict abundance based on these factors as a measure to inform the implementation of preventive actions.

2. Materials and methods

2.1. Collection sites

Traps were placed in the urban area of Palermo (Southern Italy) within the boundaries of the "Istituto Zooprofilattico Sperimentale della Sicilia" (IZSSi) (Fig. 1). From July 2009 to May 2016, a trap was placed in a collection site closed to the Laboratory of Entomology (S_1). This site is close to a tiny garden with good maintenance and without water stagnation (Fig. 1). From 2012 to 2016, additional traps were located at other four different sites covering an area of 2 ha within the IZSSi (Fig. 1). The site no. 2 (S_2) has similar characteristics to S_1. Sites no. 3 (S_3) and no. 4 (S_4) are placed at the end of ramps to access buildings, in shady paved floors (Fig. 1). Site no. 5 (S_5) is located in a small green area, near a plant nursery. A large, irrigated vegetable garden limits with IZSSi to the East.

2.2. Sampling

Sampling was carried out using commercial BG-Sentinel traps (Fig. 1) baited with the BG-Lure® artificial human scent attractant (Biogents, Regensburg, Germany). According to the manufacturer, the BG-Sentinel traps are considered the gold standard method for monitoring the vectors of dengue, chikungunya, zika and yellow fever such as *Ae. aegypti*, *Ae. albopictus* and *Ae. polynesiensis* (https://eu.biogents.com/bg-sentinel/). Traps were operated continuously, and captures were collected three times a week. The collected insects were transported to the laboratory where they were killed by freezing at −20 °C and preserved at −80 °C before identification. Mosquitoes from each capture were counted and identified according to their morphological features (Stojanovich and Scott, 1997; Severini et al., 2009; Severini et al., 2022) using reflected light stereo microscope. In particular, *Ae. albopictus* adults show the body covered with dark scales and the mesonotum with a narrow mid-longitudinal band of silvery-white scales tapering posteriorly. The claws are simple, while the abdomen has spots of white scales on the sides of each tergite and a transverse-basal band of white scales very thin or even interrupted in the middle (Severini et al., 2009). Week counts of adult *Ae. albopictus* were estimated as the sum of the captures from Monday night to Sunday night of every capture week of the study period and employed for modelling.

Table 1
Weather predictor selected for modelling, description, abbreviations employed in the text and other tables and descriptive parameters (range, average and associated standard error (SD)). *All covariates were transformed with natural logarithms. All weather covariates were estimated at either the specific week of each capture or at different time lags before the week of the capture. Only the specific time lags identified by cross-correlation matrices were included in modelling and in this table.

Predictor abbreviation	Description (units)*	Range	Average ± SD
lnwt	Average of daily mean air temperature values in the week (°C)	7.8–29.5	19.0±5.6
lnwtv	Variation of daily mean air temperature values in the week (%)	0.1–23.0	2.7±3.3
lnwp	Precipitation accumulated over the week (mm)	0.0–165.2	15.7 ±24.8
lnwpv	Variation in daily total precipitation records in the week (%)	0.0–980.2	37.6 ±98.2
lnwrh	Average air relative humidity obtained from daily records during the week (%)	39.0–75.0	59.7±6.3
lnwrhv	Variation in daily records of air relative humidity in the week (%)	0.0–308.6	49.6 ±39.1
lnwsd	Average of daily estimates of vapor pressure deficit in the week (mm)	2.5–19.2	7.2±3.4
lnwsdv	Variation in daily estimates of vapor pressure deficit in the week (%)	0.0–39.2	3.3±4.4
lnwws	Average of daily records in the week of mean wind speed (m/s)	2.5–11.1	6.4±1.4
lnwwsv	Variation in daily records of mean wind speed in the week (%)	0.1–30.2	4.1±4.4
$lnt_{(6, 1)}$	Average of daily mean air temperature values in the six weeks before capture (°C)	9.9–28.7	19.0±5.4
$lntv_{(7, 1)}$	Variation in daily records of mean temperature along the seven weeks before capture (%)	0.0–0.3	0.1±0.1
$lnp_{(14, 3)}$	Precipitation accumulated between weeks 3 and 14 before capture (mm)	1.8–587.8	171.9 ±129.3
$lnpv_{(12, 1)}$	Variation in daily records of precipitation over the 12 weeks before capture (%)	1.5–8.6	3.4±1.6
$lnrh_{(13, 2)}$	Average air relative humidity from daily values from weeks 2 to 13 before capture (%)	50.0–69.0	59.8±4.4
$lnrhv_{(19, 1)}$	Variation in daily records of air relative humidity along 19 weeks before capture (%)	0.10–0.19	0.10 ±0.02
$lnsd_{(8, 1)}$	Average vapor pressure deficit from daily estimates along 8 weeks before capture (mm)	3.2–14.7	7.3±3.1
$lnsdv_{(10, 1)}$	Variation in daily vapor pressure deficit estimates for the ten weeks before capture (%)	0.2–0.6	0.3±0.1
$lnws_{(7, 1)}$	Average speed of the wind from daily records in the seven weeks before capture (m/s)	4.4–8.8	6.3±0.8
$lnwsv_{(14, 1)}$	Variation in daily records of wind speed along the fourteen weeks before capture (%)	0.2–0.5	0.3±0.1

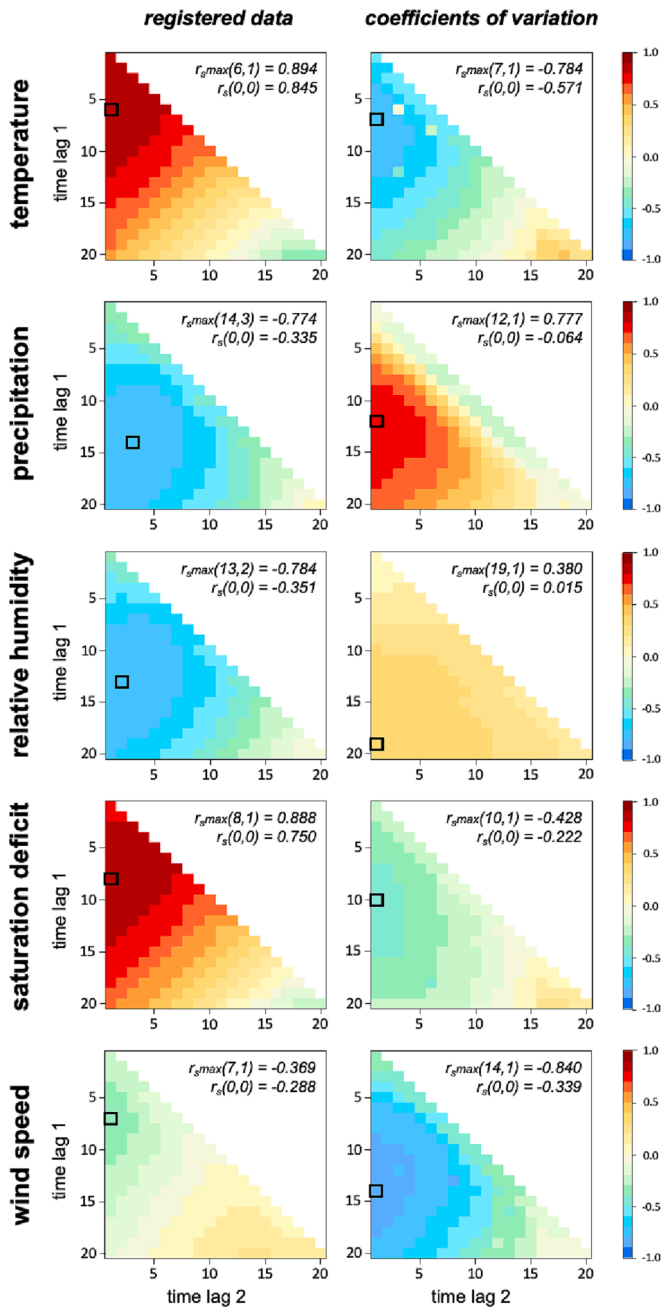

Fig. 2. Cross-correlation maps showing the Spearman rank order correlation of *Aedes albopictus* weekly captures with weather records on average temperature (°C), accumulated precipitation (mm), average air relative humidity (%), average saturation deficit (mm) and average wind speed (m/s) at 2 m height from the surface as well as with the variation in these weather parameters (measured as the coefficient of variation of daily records for the respective period). For each map, the maximum of the lagged correlation coefficients (r_s) observed and the time lag at which it was observed (lag1, lag2) is shown and additionally highlighted with a black frame. The correlation coefficient of *Ae. albopictus* abundance with weather quantities at time lag 0 (0,0) is also given per map.

2.3. Weather data

Raw weather data were obtained from Servizio Informativo Agrometeorologico Siciliano SIAS (http://www.sias.regione.sicilia.it/), taking into consideration the data of nearest station located in Palermo (Lat.: 38.129799°, Long.:13.327593°). Raw weather data obtained from the meteorological station contained daily records of minimum/maximum/average air temperature (T; °C), accumulated rainfall (P; mm), minimum/maximum/average air relative humidity (RH; %), average daily wind speed at 2 m above land surface (WS; m/s), accumulated solar radiation (SR; MJ/mq) and atmospheric pressure (AP; hPa). *Aedes albopictus* counts were modelled on a weekly basis, so weather daily records were set to the week basis (Monday-Sunday) by averaging (arithmetic mean) daily automatic registers of T, RH and WS, and by summing up daily records of P. Daily average temperature and relative humidity data were employed to estimate a week average of the drying power of the air by calculating the vapor pressure deficit (VPD) (Prenger and Ling, 2000; Seager et al., 2015). VPD represents the force for water evaporation from a land surface to the atmosphere (air drying potential) and thus it may represent a relevant correlate for both mosquito breeding favourability as well as activity, and it's been shown a relevant parameter to model mosquito-borne disease outbreak probability (Davis et al., 2018). To compute VPD we first estimated vapour saturation pressure (*vsp*) as

$$vsp = e^{\frac{A}{T}+B+CT+DT^2+ET^2+F\ln T},$$

where A = -1.88×10^4, B = -13.1, C = -1.5×10^{-2}, D = 8×10^{-7}, E = -1.69×10^{-11}, F = 6.456 and T = Temperature of the air in K. We thereafter computed actual vapour pressure (*avp*) using air RH as

$$avp = vsp \times \mathrm{RH}/100.$$

Finally, VPD was estimated as the difference between *vsp* and *avp* and expressed in kPa.

Weather variations may better shape population changes of arthropod vectors than mean (average) values of weather quantities (Poh et al., 2019) as predicted from the Schmalhuasen's law on drivers of biological systems. On this principle, we built covariates gathering the weekly variation in mean daily weather values by estimating the coefficient of variation (standard deviation divided by the mean in %) of the records of T, RH, WS, P and VPD (Table 1).

2.4. Weather correlates of Ae. albopictus abundance

The association of time lagged environmental weather quantities (and their variation) to the weekly dynamics of *Ae. albopictus* abundance was explored by cross-correlation matrices, a useful method to visualize lagged weather effects on mosquito abundance (Curriero et al., 2005). Cross-correlation matrices gather the bivariate relationships of a time series response variable (e.g., mosquito abundance) with time series explanatory variables (e.g., weather quantities) by allowing the lag effect of the explanatory variable to extend over different time periods of variable length with respect a given time of the response variable (see Groen et al. 2017). In other words, it allows us to explore for a predictor variable which past time periods are most associated with the focal (weekly) abundance of *Ae. albopictus* (our study phenomenon), and thus maximise both the ability to find the best predictors of the abundance of the species and the predictive capabilities of the model. Spearman's rank order correlations between *Ae. albopictus* abundance (non-gaussian distribution) and weather conditions for a given period and time lag were displayed as cross-correlation maps (Fig. 2). The weather variables analysed were temperature, rainfall, relative humidity, water saturation deficit and wind speed, including both the weekly average (or sum for P) of net daily records of these variables and the variation in their daily records as detailed in section 2.4 (Fig. 2). Time lags were expressed in weeks and the maximum lag considered was 20 weeks.

2.5. Predictive modelling

2.5.1. Time series modelling

The first stage in data analysis for predictive model building was to explore time series data on mosquito abundance. A time series may be structured by three components: i) trend; ii) seasonality; and iii) random

Table 2
List of weather covariates considered as predictors for Poisson regression modelling in each of the five sets of regression models of *Aedes albopictus* abundance. The whole list of covariates (and their acronyms) considered for modelling purposes in this study is shown in Table 1. WR: capture week raw (averaged or summed) record; WV: coefficient of variation of capture week daily records; TLR: time lagged raw records (averaged or summed) of the maximum observed lagged correlations; TLV: coefficient of variation of daily records of weather parameters for the maximum time lagged correlation coefficients observed.

Weather covariates	Covariate type	Model set 1 (MS1)	Model set 2 (MS_2)	Model set 3 (MS_3)	Model set 4 (MS_4)	Model set 5 (MS_5)
lnwt	WR	✓	✓			✓
lnwtv	WV	✓		✓	✓	✓
lnwp	WR	✓	✓		✓	✓
lnwpv	WV	✓		✓		✓
lnwrh	WR	✓	✓			✓
lnwrhv	WV	✓		✓	✓	✓
lnwsd	WR	✓	✓		✓	✓
lnwsdv	WV	✓		✓	✓	✓
lnwws	WR	✓	✓		✓	✓
lnwwsv	WV	✓		✓		✓
$lnt_{(6,\ 1)}$	TLR		✓			✓
$lntv_{(7,\ 1)}$	TLV			✓		✓
$lnp_{(14,\ 3)}$	TLR		✓		✓	✓
$lnpv_{(12,\ 1)}$	TLV			✓		✓
$lnrh_{(13,\ 2)}$	TLR		✓			✓
$lnrhv_{(19,\ 1)}$	TLV			✓	✓	✓
$lnsd_{(8,\ 1)}$	TLR		✓			✓
$lnsdv_{(10,\ 1)}$	TLV			✓	✓	✓
$lnws_{(7,\ 1)}$	TLR		✓		✓	✓
$lnwsv_{(14,\ 1)}$	TLV			✓		✓

variation. The time series data on *Ae. albopictus* weekly captures at S_1 was decomposed in components using the 'decompose' function of the 'stats' package of R (R v4.1.3; R Core Team, 2012) to estimate whether data are non-stationary (trend), present a seasonal component and to estimate the random variation on captures. The autocorrelation function (ACF) and the partial autocorrelation function (PACF) of the time series mosquito counts were estimated ('stats' package of R) to assess the autocorrelation of the captures at different time lags. The PACF informs about the order of the autoregressive (AR) process of time series data (**p**) whereas the ACF gives the value of the moving average (MA) model (**q**) that represents the lag above which autocorrelation of the time series is no further significant. An additional component of the function that estimates a value of the time series at a given time is represented by the integration (I) parameter (**d**). This parameter indicates the number of differences between consecutive observations that are required to make the time series stationary, i.e., to remove the non-constant trend of the series.

For modelling purposes, the diversity of scales of weather covariates (and coefficients of variation) was homogenised by $\log_e(x)$ transformation. The 7-year dataset obtained in S_1 was the most appropriate for modelling *Ae. albopictus* abundance as it was the most complete time series of the five data series obtained in S_1 to S_5. We first fitted a SARIMA model to the time series data of *Ae. albopictus* captures. The model was extended by introducing weather covariates using a forward stepwise procedure, retaining covariates included in models with the lowest conditional Akaike Information Criterion (cAIC). Time lagged weather covariates that showed the highest correlations with mosquito abundance in the cross-correlation maps were also included in the SARIMA models (see Table 1). SARIMA models were built using the 'auto.arima' function of the R 'forecast' package (Hyndman and Khandakar, 2008). This function searches through combinations of order parameters and chooses the set that optimises the model fit criteria.

2.5.2. Poisson linear regression modelling

As one of our aims was understanding the influential role of specific weather parameters on *Ae. albopictus* demographic patterns, that's inference, we undertook a thorough data exploration as suggested by Zuur et al. (2010) to overcome the influential effect of outliers, ensure balance and, above all, explore the relationships among covariates and remove collinearity (Supplementary Fig. 1; see Casades-Martí et al., 2020 for more details on the exploratory analysis). Lebl et al. (2013) achieved good accuracy in *Culex pipiens/restuans* forecasting approaches with Poisson regression over 20 years of captures in Chicago. Five sets of Poisson regression models were built using the'glm' function of the 'stats' package of R: i) Model set 1 (MS_1) was conducted using only the weather conditions (raw records and coefficients of variation) for the week of mosquito trapping; ii) Model set 2 (MS_2) used the week and period (time lagged) weather conditions (maximum correlations per parameter identified with CCMs) excluding estimates of weather variation; iii) Model set 3 (MS_3) was constructed only with the covariates capturing the variation in weather conditions for the catch week and the lagged time periods showing the highest correlations with catches; iv) Model set 4 (MS_4) included only the uncorrelated covariates of week and time lagged weather identified in the exploratory analysis; and v) Model set 5 (MS_5) was constructed as the over-saturated model that included week and time lagged selected covariates (both raw records and variation). To better explain the modelling approach, Table 2 shows the covariates included in each model set.

All possible models in each set of models were constructed and ranked using the increasing conditional Akaike information criterion (cAIC) with the 'dredge' function of the R statistical package 'MuMIn' (Barton 2009). Those models showing a difference of <2 units in the cAIC with respect to the model with the lowest cAIC (ΔcAIC <2; Supplementary Table 1) were selected for model averaging with the 'model.avg' function of the 'MuMIn' package. The occurrence and influence of multicollinearity was checked by estimating the variance inflation factor (VIF; 'vif' function of R 'car' package) of the best fitted model in every model set.

2.5.3. Model validation and predictive capacity

For the validation of the predictive capacity of the models, we followed a two-pronged approach. First, we performed an internal validation based on the partitioning of the S_1 data into a training dataset, on which we built the models, and a validation or test dataset, on which we validated them. Secondly, after assessing the predictive capacity of the different models (SARIMA and Poisson regression models), the model with the best predictive capacity and whose predictions were best adjusted to the observed seasonality of *Ae. albopictus* (Fig. 3), was externally (out-of-sample) assessed using the most temporally limited capture data (2012–2016) from traps S_2 to S_5.

For the first stage of model validation, the data from the S_1 trap dataset were divided into different training and test datasets. For the internal validation of the temporally explicit models (SARIMA), and since this must be done prospectively (Hu et al., 2006), the training dataset included the catches of the first five years of the series (week 27, 2009 to week 26, 2014) while data of the last two years (week 27, 2014 to week 29, 2016) were left for the test dataset. The predictive potential of best-fit SARIMA model on train dataset (including covariates) was estimated as the fit to test dataset based on the root mean square error (RMSE), a parameter that allows comparing models from different model sets while controlling the effects of possible large errors in predicted versus observed values. For the internal validation of the Poisson regression models, we used several options for partitioning the S_1 data into training and test data: i) the same as described for the validation of the SARIMA models; ii) one in which odd years were used as training and even years as test (Lebl et al., 2013); and iii) random partitions of the data in training-to-test ratios 60:40 and 50:50. The predictive potential of the best-fit Poisson regression models was estimated on the test dataset using the 'predict' function of the R package 'stats'. The RMSE

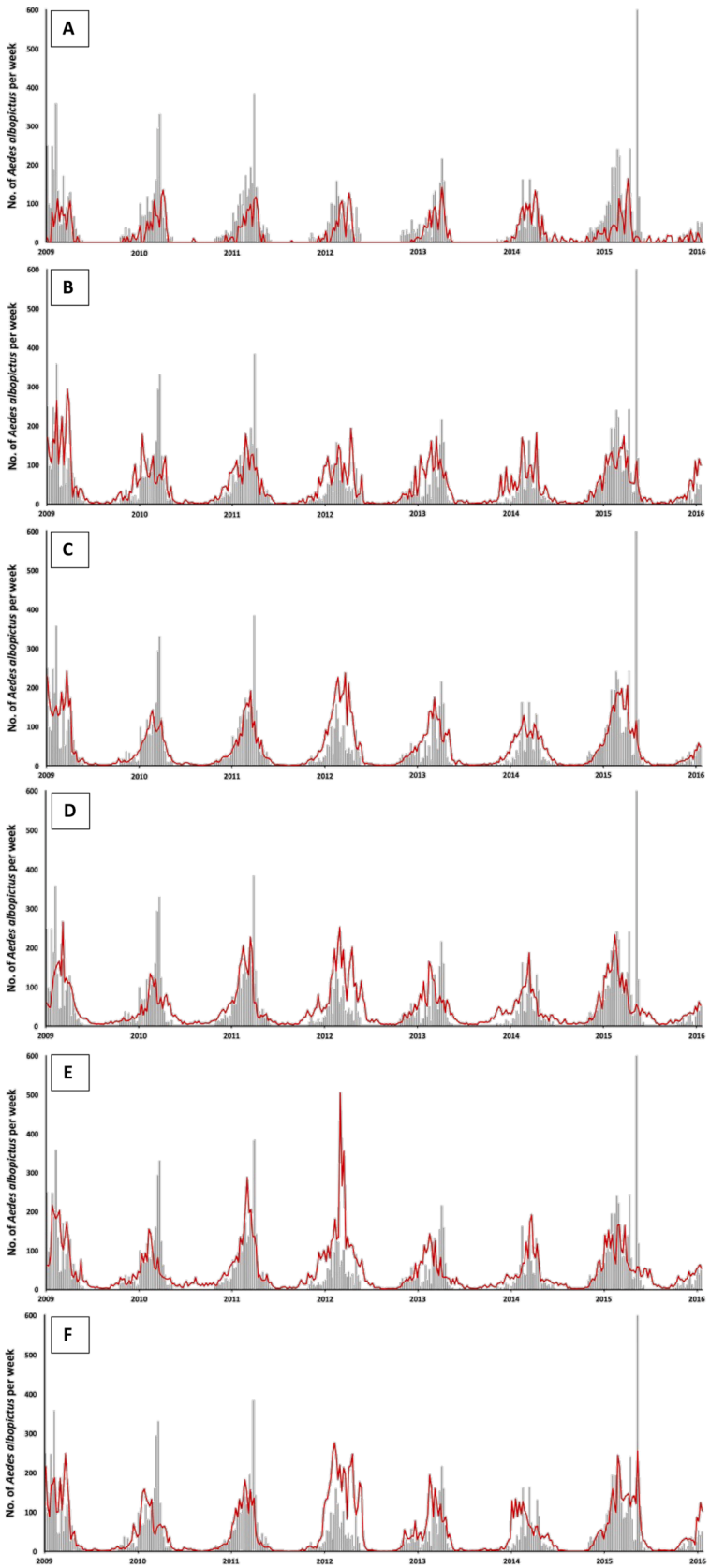

Fig. 3. Temporal dynamics of observed (gray bars) *vs.* predicted (red line) numbers of *Aedes albopictus* along the study period in S_1. Predicted numbers were based on best SARIMA model (A) and Poisson regression model sets MS_1 (B), MS_2 (C), MS_3 (D), MS_4 (E) and MS_5 (F). Negative predicted values were truncated to 0 for plotting.

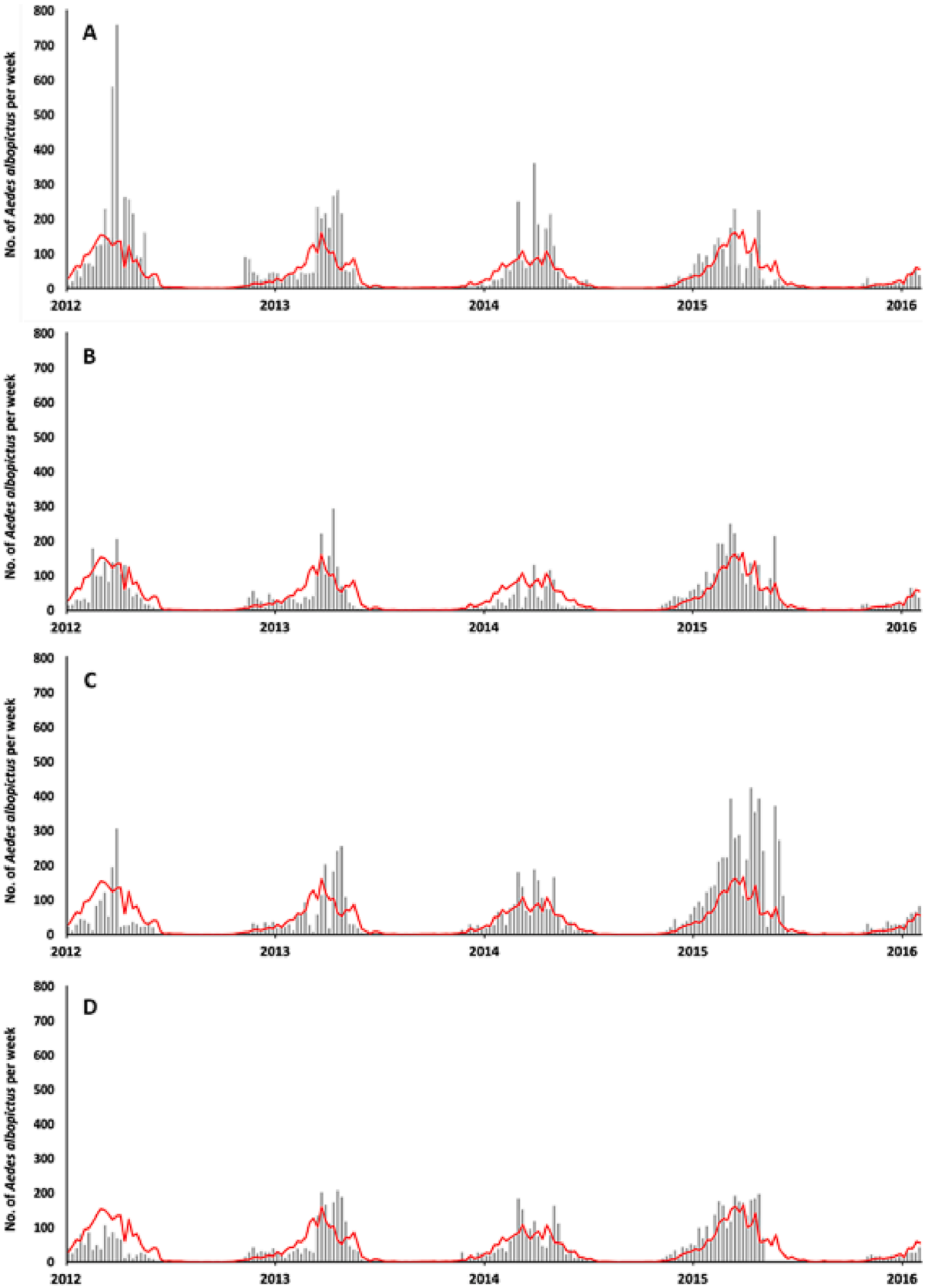

Fig. 4. Weekly number of *Aedes albopictus* predicted by the best fitted Poisson regression model of MS_2 over total captures in S_1 (red line) *vs.* observed numbers (grey bars) in S_2 (A), S_3 (B), S_4 (C) and S_5 (D) from week 25, 2012 to week 29, 2016.

Table 3
Best fitted seasonal ARIMA model with order (p, d, q)(P, D, Q). The coefficients of different orders of the autoregressive parameter (p), the seasonal autoregressive parameter (P) and regressors and their standard errors (in brackets) are displayed.

p		P		Regressors	RMSE
Order	Coefficient	Order	Coefficient	Coefficient	
1	−0.380 (0.068)	1	−0.547 (0.064)	−7.623 (2.228)	42.980
2	−0.244 (0.072)				
3	−0.267 (0.069)				

was again the parameter used to estimate internal model performance. Comparison of the predictive potential of the best-fit model in each of the five Poisson regression model sets and the SARIMA model based on RMSE allowed us to select the best model for predicting *Ae. albopictus* abundance in our study area. The external validation allowed us to test the out-of-sample performance of the selected model.

3. Results

3.1. Mosquito monitoring results

From 2009 to 2016, 18,830 Culicidae were collected in S_1. Out of them, 12,152 (65%) were *Ae. albopictus* and the remaining 6,678 (35%) belonged to the *Culex* and *Culiseta* genera. From 2012 to 2016, an additional burden of 58,710 mosquitoes (33,094 (56%) *Ae. albopictus* and 25,616 (44%) *Culex* and *Culiseta* ssp. spp.) were captured in S_2-to-S_5. The abundance of *Ae. albopictus* was highly seasonal (Figs. 3 and 4). These were active between mid-March and late-December, and they were very abundant between July and September (Supplementary Fig. 2). The highest abundance peaks (over 600 captures in a week) were however observed in Autumn (week 45 in S_1 and week 41 in S_2; Figs. 3 and 4). No activity was recorded between weeks 1 to 12 (January to mid-March) (Supplementary Fig. 2).

3.2. Weather correlates of Ae. albopictus abundance

No clear seasonality was observed in wind speed. Temperatures spiked in summer, consequently causing downward spikes in relative air humidity. Relative humidity was however relatively constant along the year (range 39–75%), most probably caused by the proximity to the coast of IZSSi (4 km inland in a straight line; Fig. 1). Rainfall was almost absent in summer; it mainly accumulated over the autumn and winter as typically reported for Mediterranean climates. The VPD seasonality highly resembled that of temperatures as far as the seasonal variation in relative humidity was more limited. The temporal dynamics of weather quantities is displayed in Supplementary Figs. 3 and 4.

The weekly abundance of *Ae. albopictus* was strongly positively correlated with air temperature ($r_s(0,0) = 0.845$) and VPD ($r_s(0,0) = 0.750$) of the capture week (Fig. 2). The correlations with the accumulated precipitation ($r_s(0,0) = -0.335$), air relative humidity ($r_s(0,0) = -0.351$) and wind speed ($r_s(0,0) = -0.288$) in the week of the capture were negative but weak. Variations in weather quantities in the week of capture were irrelevant in shaping *Ae. albopictus* abundance, with the exception of a weak negative effect ($r_s(0,0) = -0.571$) of the variations in average air temperature values. Mimicking the observed effect of the capture week, lagged values of average temperature ($r_s(6,1) = 0.894$) and VPD ($r_s(8,1) = 0.888$) were also strongly positively correlated with *Ae. albopictus* abundance. Negative associations stronger than those observed for weather quantities of the capture week were observed for the accumulated precipitation ($r_s(14,3) = -0.774$) and air relative humidity ($r_s(13,2) = -0.784$) along periods of 3–4 months before abundance estimates. No relationship was found with wind speed. The observed effects of the variation in weather quantities were, in contrast to the values recorded in the week of capture, stronger for time lagged weather variation quantities of temperature ($r_s(7,1) = -0.784$), precipitation ($r_s(12,1) = 0.777$) and wind speed ($r_s(14,1) = -0.840$).

3.3. SARIMA models

The best-fit most parsimonious seasonal ARIMA model ((3, 1, 0)(1, 1, 0)[52]) (Table 3) included the variation in air temperature of the week of capture, the precipitation accumulated along weeks 3–14 before capture and the variation in air relative humidity during the previous 4.5 months (19 weeks). The selected SARIMA model was able to accurately predict seasonality in *Ae. albopictus* abundance (Fig. 3A). This model overpredicted out-of-season abundance of *Ae. albopictus* for the last two years even though it generally was under predictive (Fig. 3), especially during the main season of *Ae. albopictus* activity. The SARIMA model was unable to capture abundance peaks that stochastically occurred in S_1 along the years (Fig. 3 & Supplementary Fig. 5).

3.4. Poisson regression models

Validation based on partitioning the data into odd and even years resulted in the lowest RMSE values and was considered optimal for the Poisson regression models. Best-fit models from MS_1 and MS_2 better adjusted predictions to observations than the other Poisson regression model sets. Both models had a similar predictive capacity that was also very close to the predictive potential of the best fitted SARIMA model (Table 3). Both model sets were accurate in predicting the activity session of *Ae. albopictus*, but the selected model from MS_2 displayed a higher accuracy in predicting seasonality (Fig. 3C), i.e., to predict the periods at which *Ae. albopictus* were inactive, than best fitted SARIMA and MS_1 models. This model additionally displayed a good ability to predict interannual variations in abundance within the main activity season of the mosquito in contrast to best-fit SARIMA and MS_1 models (Fig. 3). The evidence of a higher performance of best-fit model from MS_2 was the reason behind its election to test its ability to predict *Ae. albopictus* abundance out-of-sample in S_2-to-S_5. The model was accurate in predicting abundance at S_3 and S_5 (RMSE = 33.321 and RMSE = 34.548, respectively) but it was underpredicting abundance in S_2 and S_4 (RMSE = 72.402 and RMSE = 63.972, respectively) (Fig. 4). Model set no. 4 (MS_4) was built upon non-correlated (independent) explanatory covariates to allow inferring relevant associations of weather quantities with *Ae. albopictus* abundance (Table 2). The correlation matrix of weather covariates is shown in the Supplementary Fig. 1. The variation in air relative humidity along the 4.5 months before the capture and the VPD of the capture week were positive determinants of *Ae. albopictus* abundance (Table 4). Wind speed values in the week of capture as well as time lagged values were the most relevant negative drivers of *Ae. albopictus* abundance. The VIF remained below 10 for the predictors selected in this model (Table 4).

4. Discussion

Predictive modelling is a highly useful tool to efficiently manage vector populations and prevent vector-borne pathogen transmission (Bationo et al., 2021). Actions taken based on reliable predictions not only may inform managers to apply pesticides at specific times to reduce environmental contamination, but also may inform to opt for less environmentally impactful alternatives within and integrated pest management strategy (Albertson & Sequeira, 2018), and it finally improves the efficiency of the methods and reduces the associated costs. This has a tremendously relevant impact at both local and regional scales, so predictive models need to be highly accurate to be useful. We opted for SARIMA and Poisson models, but there are other equally accurate approaches to predict the spatiotemporal dynamics of vector abundance (e.g., Chen et al., 2019). Both the best Poisson regression model and the SARIMA model showed similar predictive capabilities. However, we observed that the selected Poisson regression model more

Table 4
Output of average Poisson regression models – included predictors, estimates, the standard error associated with the estimate (SE), the statistic (z) and the p-value – from any of the five sets of models performed. Results of the goodness of fit – estimated error (RMSE) – and variance inflation factor (VIF) are also presented. *$p < 0.05$, **$p < 0.01$, ***$p < 0.001$.

Model set	Predictor	Estimate	SE	z	p	VIF	RMSE
MS_1	*Intercept*	*−15.6288*	*0.9422*	*16.474*	***		43.059
	lnwp	0.3149	0.0291	10.744	***	22.849	
	lnwt	6.5842	0.1638	39.922	***	28.899	
	lnwrh	1.0963	0.2336	4.661	***	21.671	
	lnwsdv	−0.3914	0.0195	19.905	***	8.356	
	lnwws	−3.0165	0.1035	28.927	***	3.099	
	lnwpv	−0.0935	0.0219	4.248	***	20.647	
	lnwtv	0.0836	0.0139	5.963	***	2.244	
	lnwwsv	0.2161	0.0138	15.515	***	3.135	
	lnwsd	0.0148	0.1124	0.131	0.896	79.376	
	lnwrhv	0.0017	0.0140	0.119	0.905	5.224	
MS_2	*Intercept*	*11.0126*	*2.5028*	*4.370*	***		43.039
	lnwsd	−3.1551	0.2491	12.579	***	80.345	
	lnwp	−0.0457	0.0104	4.373	***	2.737	
	$lnp_{(14, 3)}$	0.0806	0.0120	6.669	***	2.117	
	$lnrh_{(13, 2)}$	−1.7020	0.4486	3.768	***	4.984	
	$lnsd_{(8, 1)}$	2.9661	0.1269	23.232	***	11.949	
	lnwt	4.5456	0.3233	13.963	***	30.723	
	lnwrh	−2.7884	0.4386	6.313	***	22.229	
	lnwws	−0.7246	0.0850	8.463	***	2.001	
	$lnws_{(7,1)}$	−1.0875	0.1978	5.459	***	2.565	
	$lnt_{(6, 1)}$	0.0844	0.1908	0.441	0.660	13.525	
MS_3	*Intercept*	*6.7114*	*0.2327*	*28.634*	***		46.967
	$lnrhv_{(19, 1)}$	3.2072	0.1225	26.000	***	1.289	
	$lnsdv_{(10, 1)}$	0.2752	0.0742	3.684	***	2.350	
	$lntv_{(7, 1)}$	−1.0075	0.0448	22.341	***	3.893	
	$lnwsv_{(14, 1)}$	−1.8429	0.0814	22.500	***	3.687	
	lnwsdv	0.0523	0.0208	2.500	*	4.676	
	lnwpv	0.0722	0.0063	11.429	***	1.604	
	lnwrhv	−0.2908	0.0252	11.468	***	3.614	
	lnwwsv	−0.1018	0.0099	10.168	***	1.872	
	lnwtv	0.0098	0.0138	0.713	0.476	2.164	
	$lnpv_{(12, 1)}$	0.0181	0.0392	0.459	0.646	3.914	
MS_4	*Intercept*	*16.7010*	*0.3865*	*42.913*	***		58.176
	$lnrhv_{(19, 1)}$	3.2429	0.1273	25.289	***	1.310	
	lnwsd	1.2020	0.0544	21.955	***	6.414	
	$lnp_{(14, 3)}$	−0.4538	0.0105	43.100	***	2.452	
	lnwsdv	−0.1553	0.0222	6.951	***	8.799	
	lnwws	−1.8147	0.0712	25.299	***	1.625	
	lnwtv	0.1338	0.0127	10.434	***	2.010	

Model set	Predictor	Estimate	SE	z	p	VIF	RMSE
MS_4	$lnws_{(7,1)}$	−2.1334	0.1330	15.931	***	1.369	58.176
	lnwp	0.0048	0.0005	10.145	***	1.895	
	lnwrhv	−0.0083	0.0207	0.400	0.689	5.212	
	$lnsdv_{(10, 1)}$	−0.0092	0.0371	0.245	0.806	2.368	
MS_5	*Intercept*	*−8.8512*	*3.1177*	*2.822*	**		59.565
	$lnpv_{(12, 1)}$	−0.2210	0.0668	3.286	**	6.256	
	$lnsdv_{(10, 1)}$	2.4640	0.0925	26.444	***	4.257	
	$lntv_{(7, 1)}$	−0.2946	0.0619	4.722	***	5.399	
	$lnwsv_{(14, 1)}$	1.5789	0.1316	11.912	***	7.012	
	lnwsd	−2.3571	0.2824	8.287	***	110.988	
	lnwp	−0.1293	0.0326	3.943	***	28.347	
	$lnp_{(14, 3)}$	−0.1014	0.0183	5.517	***	4.982	
	$lnrh_{(13, 2)}$	1.4145	0.5533	2.541	*	6.898	
	$lnsd_{(8, 1)}$	3.6225	0.1729	20.802	***	16.732	
	$lnt_{(6, 1)}$	1.5550	0.3036	5.084	***	17.247	
	lnwt	4.7480	0.3762	12.529	***	39.224	
	lnwrh	−1.6586	0.4886	3.370	***	29.919	
	lnwws	−1.5647	0.1282	12.113	***	4.930	
	lnwpv	0.1124	0.0238	4.687	***	24.021	
	lnwtv	0.0292	0.0187	1.558	0.119	2.812	
	lnwrhv	−0.1314	0.0235	5.566	***	6.361	
	lnwwsv	0.1309	0.0156	8.360	***	4.021	
	$lnws_{(7,1)}$	−0.2135	0.2478	0.859	0.390	2.920	
	lnwsdv	−0.0035	0.0150	0.230	0.818	11.373	
	$lnrhv_{(19, 1)}$	−0.0149	0.0690	0.215	0.830	2.136	

accurately fit the seasonality of abundance as well as abundance point peaks. Whereas the MS_2 Poisson regression model tended to overpredict abundance within the observed window of *Ae. albopictus* activity, the SARIMA model was under predictive, thus showing the better fit of the selected Poisson model at similar prediction error rates. This indicates that even though both approaches are equally valid in terms of predictive ability, the Poisson model would offer higher predictive accuracy at smaller time scales (such as one week) and out of the main mosquito activity season than the SARIMA model. Further, the predictive performance of the best fitted Poisson model for S_1 capture data was highly accurate in terms of seasonal activity prediction for traps S_2 to S_4, thus corroborating its predictive potential and usefulness.

For the selected region, the study was conducted in a circumscribed urban context to characterize mosquito abundance at a local scale. The site selected for the study is representative not only for the city of Palermo, but also for urban areas where *Ae. albopictus* has become stablished at the Mediterranean Basin (Petrić et al., 2021). To our knowledge, this study is unique in that it investigates the abiotic environmental drivers of *Ae. albopictus* population dynamics with a comprehensive longitudinal survey in a Mediterranean urban area. Our results are consistent with those obtained in a recent study (Manica et al., 2016) conducted out in metropolitan and sub-urban/rural areas of Rome (Italy). In that study, adult mosquitoes were followed longitudinally along a 70 km routethrough and beyond the most urbanised and densely populated metropolitan area. The authors found that hotspots of *Ae. albopictus* abundance within highly anthropised Metropolitan stations are associated with "small green islands" that may represent ideal sites in which the mosquito finds optimal conditions for egg-laying and resting.

The weekly dynamics of the species in S_1 over seven years showed a uniform seasonality, which clearly manifests that the species is well adapted to local conditions (Bella et al., 2018). However, Mediterranean winter conditions restrict their activity when average weekly temperatures fall below 15 °C, which contrasts with their continued activity in original tropical areas (e.g., Zheng et al., 2019). In coastal areas, where winter conditions are buffered by sea water, the period of inactivity is short (December-March), but in inland areas activity may be reduced to the most favourable season (May-October). The main determinants of both seasonal activity and abundance of *Ae. albopictus* in Mediterranean coastal areas are predominantly weather conditions, as observed in previous studies (e.g, Roiz et al., 2010). We did not focus attention to the influence of variations in host abundance due to the high availability of hosts for *Ae. albopictus* (Little et al., 2022) both in and around IZSSi, but, at local spatial scales, host availability influences *Ae. albopictus* abundance (Yang et al., 2021). In humanised Mediterranean environments the activity and abundance of the species are strongly associated with both actual and recent weather conditions due to the temporal dependence of point abundance estimates on the previous status of the population. This is derived from the accumulation of favourable conditions for activity and survival of adults, reproduction, and development of larvae (Farjana et al., 2012). This triggers a clear seasonality along the Mediterranean shores (e.g., Tran et al., 2013; Bella et al., 2018). In coastal areas, air moisture is fairly stable throughout the year and temperature variations are buffered by the proximity of the sea. Thus, we observed a very positive effect of VPD and RH variation on abundance, indirectly indicating the relevance of T in *Ae. albopictus* dynamics. Urban environments offer availability of water for larval development, so the dynamics of the species was found to be independent of the local rainfall regime. We expected winds to modulate activity, not abundance, and therefore weekly catches, and this was corroborated according to MS_4 output. The negative effect of constant strong winds over a larger period before captures seems to have more to do with the local wind regime; stronger winds occur in the coldest months, when temperatures are below the required threshold for the species to be active, whereas warmer months are dominated by anticyclonic, less windy, conditions. A relevant parameter modulating environmental favourability for *Ae. albopictus* is VPD, which in our study conditions we deem to be reflecting a clear effect of T in an environment where air moisture remains high along the year. Thus, although a positive effect was observed in our study area, we would predict that the colonisation of the vast amplitude of Mediterranean regions with a favourable temperature pattern for the species would be conditioned by the amount of air moisture in these regions. However, urban environments could offer favourable conditions for the species to settle there, with the consequent local risk for the whole area of Mediterranean climatic influence. The species has currently colonised some urban areas in continental Mediterranean regions (Lucientes et al., 2019), but not large continental rural areas of the Iberian Peninsula (Durán-Martínez et al., 2012; Bravo-Barriga et al., 2021) or high altitudes in inner Italian Peninsula (Romiti et al., 2022). However, the relentless increase of urban areas in Europe would favour the presence of the species in a greater number of urban environments in the Mediterranean Basin (Li et al., 2014). In urban continental areas, even though high hydric stress may condition the survival of *Ae. albopictus* during the driest season, the species could be active in wetter and still warm seasons, e.g., spring and autumn. Weather pulses of precipitation interspersed within highly favourable windows of temperature for *Ae. albopictus*, e.g., storms, may also favour breeding pulses of the species and a lower but not negligible risk of pathogen spread with these premises. Thus, the whole urban areas of southern and central Europe could be colonized by *Ae. albopictus* in the near future, being additionally favoured by increasing global temperatures (European Centre for Disease Control, 2009). CCMs showed that weather quantities over periods of length (exceeding the expected average survival time of adult *Ae. albopictus* (Cui et al., 2021)) were relevant drivers of the overall population across different generations. This resembles findings of drivers of *Culex* mosquitoes (Lebl et al., 2013) and it shows how relevant it is to act well in advance to annual abundance peaks to reduce *Ae. albopictus* to control their negative effects over hosts.

5. Conclusions

Information obtained in this kind of studies could address the choice of sites for monitoring plans on a large scale. Indeed, the knowledge of the ecological behaviour of the vector species of interest is essential to assess correct surveillance programs that could detect the introduction of the species of interest in an early phase when the establishment could be still prevented. Even if the only presence of a vector species in an area is not alone enough to determine the spreading of a pathogen in the area, an accurate surveillance of vector presence and expansion is surely a key factor for disease containment and prevention. Our model could have application in the early prediction of changes in *Ae. albopictus* abundance based on increasingly accurate weather forecasts and could thus have application in the pre-emptive prediction of abundance peaks that could have health implications. However, to prove its usefulness beyond the urban environment studied, our model should demonstrate similar predictive capacity to that found in our study settings in other environmentally similar regions that *Ae. albopictus* has colonised.

Declaration of Competing Interest

The authors declare that they have no known competing financial interests or personal relationships that could have appeared to influence the work reported in this paper.

Data availability

Data will be made available on request.

Acknowledgement and Funding

Research was supported by the Italian Ministry of Health (IZS SI 03/

19 RC and IZS SI 06/21 RC). The authors acknowledge funding from the Spanish Ministry for the Science and Innovation (MCI; projects CGL2017-89866-R and E-RTA2015-00002-C02-02). LC-M is funded by MCI (PEJ2018-003155-A) and AP-M acknowledges funding from the University of Castilla-La Mancha (2019-PREDUCLM-10932) and Social European Fund (EU).

Appendix A. Supplementary data

Supplementary data to this article can be found online at https://doi.org/10.1016/j.ecolind.2023.110232.

References

Albertson, J., Sequeira, J., 2018. Handbook for mosquito management on National Wildlife Refuges. U.S. Fish & Wildlife Service. https://www.fws.gov/policy/MosquitoHandbook_6_2018.pdf (accessed 29 April 2022).

Baldacchino, F., Caputo, B., Chandre, F., Drago, A., della Torre, A., Montarsi, F., Rizzoli, A., 2015. Control methods against invasive *Aedes mosquitoes* in Europe: a review. Pest Manag Sci. 71 (11), 1471–1485. https://doi.org/10.1002/ps.4044.

Bationo, C.S., Gaudart, J., Dieng, S., Cissoko, M., Taconet, P., Ouedraogo, B., Somé, A., Zongo, I., Soma, D.D., Tougri, G., Dabiré, R.K., Koffi, A., Pennetier, C., Moiroux, N., 2021. Spatio-temporal analysis and prediction of malaria cases using remote sensing meteorological data in Diébougou health district, Burkina Faso, 2016–2017. Sci Rep. 11 (1), 20027. https://doi.org/10.1038/s41598-021-99457-9.

Bella, S., Russo, A., Suma, P., 2018. Monitoring of *Aedes albopictus* (Skuse) (Diptera, Culicidae) in the city of Catania (Italy): seasonal dynamics and habitat preferences. Journal of Entomological and Acarological Research. 50, 7217. https://doi.org/10.4081/jear.2018.7217.

Bravo-Barriga, D., Gouvela de Almeida, A.P., Delacour-Estrella, S., Estrada Peña, R., Lucientes, J., Sánchez-Murillo, M., Frontera, E., 2021. Mosquito fauna in Extremadura (western Spain): Updated catalog with new records, distribution maps, and medical relevance. Journal of Vector Ecology. 46 (1), 70–82. https://doi.org/10.52707/1081-1710-46.1.70.

Casades-Martí, L., González-Barrio, D., Royo-Hernández, L., Díez-Delgado, I., Ruiz-Fons, F., 2020. Dynamics of Aujeszky's disease virus infection in wild boar in enzootic scenarios. Transbound Emerg Dis. 67 (1), 388–405. https://doi.org/10.1111/tbed.13362.

Chen, S., Whiteman, A., Li, A., Rapp, T., Delmelle, E., Chen, G., Brown, C.L., Robinson, P., Coffman, M.J., Janies, D., Dulin, M., 2019. An operational machine learning approach to predict mosquito abundance based on socioeconomic and landscape patterns. Landscape Ecology. 34, 1295–1311. https://doi.org/10.1007/s10980-019-00839-2.

Cianci, D., Hartemink, N., Zeimes, C.B., Vanwambeke, S.O., Ienco, A., Caputo, B., 2015. High Resolution Spatial Analysis of Habitat Preference of *Aedes albopictus* (Diptera: Culicidae) in an Urban Environment. J Med Entomol. 52 (3), 329–335. https://doi.org/10.1093/jme/tjv026.

Cuadrado-Matías, R., Baz-Flores, S., Peralbo-Moreno, A., Herrero-García, G., Risalde, M. A., Barroso, P., Jiménz-Ruiz, S., Ruiz-Rodríguez, C., Ruiz-Fons, F., 2022. Determinants of Crimean-Congo haemorrhagic fever virus exposure dynamics in Mediterranean environments. Transbound Emerg Dis. 69 (6), 3571–3581. https://doi.org/10.1111/tbed.14720.

Cui, G., Zhong, S., Zheng, T., Li, Z., Zhang, X., Li, C., Hemming-Schroeder, E., Zhou, G., Li, Y., 2021. *Aedes albopictus* life table: environment, food, and age dependence survivorship and reproduction in a tropical area. Parasites and Vectors. 14, 568. https://doi.org/10.1186/s13071-021-05081-x.

Curriero, F.C., Shone, S.M., Glass, G.E., 2005. Fall. Cross correlation maps: a tool for visualizing and modeling time lagged associations. Vector Borne Zoonotic Dis. 5 (3), 267–275. https://doi.org/10.1089/vbz.2005.5.267.

Davis, J.K., Vincent, G.P., Hildreth, M.B., Kightlinger, L., Carlson, C., Wimberly, M.C., 2018. Improving the prediction of arbovirus outbreaks: A comparison of climate-driven models for West Nile virus in an endemic region of the United States. Acta Trop. 185, 242–250. https://doi.org/10.1016/j.actatropica.2018.04.028.

Durán-Martínez, M., 2012. Distribución, abundancia y composicion de la comunidad de dípteros hematófagos vectores de enfermedades en Castilla – La Mancha: riesgos para la salud pública y la sanidad animal. University of Castilla –, La Mancha, Spain. PhD Thesis.

European Centre for Disease Control, 2009. Technical Report. Development of *Aedes albopictus* risk maps. Stockholm. https://www.ecdc.europa.eu/sites/default/files/media/en/publications/Publications/0905_TER_Development_of_Aedes_Albopictus_Risk_Maps.pdf. (accessed 10 May 2022).

Farjana, T., Tuno, N., Higa, Y., 2012. Effects of temperature and diet on development and interspecies competition in *Aedes aegypti* and *Aedes albopictus*. Medical and Veterinary Entomology. 26, 210–217. https://doi.org/10.1111/j.1365-2915.2011.00971.x.

Geoghegan, J.L., Walker, P.J., Duchemin, J.B., Jeanne, I., Holmes, E.C., 2014. Seasonal drivers of the epidemiology of arthropod-borne viruses in Australia. PLoS Negl Trop Dis. 20, 8(11):e3325. doi: 10.1371/journal.pntd.0003325.

Groen, T.A., L'Ambert, G., Bellini, R., Chaskopoulou, A., Petric, D., Zgomba, M., Marrama, L., Bicout, D.J., 2017. Ecology of West Nile virus across four European countries: empirical modelling of the *Culex pipiens* abundance dynamics as a function of weather. Parasite Vector. 10, 524. https://doi.org/10.1186/s13071-017-2484-y.

Hu, W., Tong, S., Mengersen, K., Oldenburg, B., 2006. Rainfall, mosquito density and the transmission of Ross River virus: A time-series forecasting model. Ecol Modelling. 196, 505–514. https://doi.org/10.1016/j.ecolmodel.2006.02.028.

Hyndman, R.J., Khandakar, Y., 2008. Automatic time series forecasting: the forecast package for R. Journal of Statistical Software. 26 (3), 1–22.

Johnson, N., Fernández de Marco, M., Giovannini, A., Ippoliti, C., Danzetta, M.L., Svartz, G., Erster, O., Groschup, M.H., Ziegler, U., Mirazimi, A., Monteil, V., Beck, C., Gonzalez, G., Lecollinet, S., Attoui, H., Moutailler, S., 2018. Emerging Mosquito-Borne Threats and the Response from European and Eastern Mediterranean Countries. Int J Environ Res Public Health. 15 (12), 2775. https://doi.org/10.3390/ijerph15122775.

Kilpatrick, A.M., Pape, W.J., 2013. Predicting human West Nile virus infections with mosquito surveillance data. Am J Epidemiol. 178 (5), 829–835. https://doi.org/10.1093/aje/kwt046.

Lebl, K., Brugger, K., Rubel, F., 2013. Predicting *Culex pipiens/restuans* population dynamics by interval lagged weather data. Parasit Vectors. 6, 129. https://doi.org/10.1186/1756-3305-6-129.

Li, Y., Kamara, F., Zhou, G., Puthiyakunnon, S., Li, C., Liu, Y., Zhou, Y., Yao, L., Yan, G., Chen, X.G., 2014. Urbanization increases *Aedes albopictus* larval habitats and accelerates mosquito development and survivorship. PLoS Negl Trop Dis. 8 (11), e3301.

Little, E.A.H., Hutchinson, M.L., Price, K.J., Marini, A., Shepard, J.J., Molaei, G., 2022. Spatiotemporal distribution, abundance, and host interactions of two invasive vectors or arboviruses, *Aedes albopictus*, and *Aedes japonicus*, in Pennsylvania, USA. Parasites and Vectors. 15, 36. https://doi.org/10.1186/s13071-022-05151-8.

Lucientes, J., Delacour Estrella, S., 2019. [Vigilancia entomológica de mosquito tigre (*Aedes albopictus*) en Aragón. Año 2019]. Report. University of Zaragoza, Spain. https://www.aragon.es/documents/20127/1650151/INFORME_2019_VIGILANCIA_ENTOMOLOGICA_DGA-6.pdf/74142f45-e5aa-63f5-08ca-ffbc054b09b0?t=1591783870386'. (accessed 29 April 2022).

Macaluso, G., Gucciardi, F., Guercio, A., Blanda, V., La Russa, F., Torina, A., Mira, F., Bella, S.D., Lastra, A., Giacchino, I., Castronovo, C., Vitale, G., Purpari, G., 2021. First neuroinvasive human case of West Nile Disease in Southern Italy: Results of the 'One Health' approach. Vet Med Sci. 7 (6), 2463–2472. https://doi.org/10.1002/vms3.591.

Manica, M., Filipponi, F., D'Alessandro, A., Screti, A., Neteler, M., Rosà, R., Solimini, A., Della Torre, A., Caputo, B., 2016. Spatial and Temporal Hot Spots of *Aedes albopictus* Abundance inside and outside a South European Metropolitan Area. PLoS Negl Trop Dis. 10 (6), e0004758.

Mercier, A., Obadia, T., Carraretto, D., Velo, E., Gabiane, G., Bino, S., Vazeille, M., Gasperi, G., Dauga, C., Malacrida, A.R., Reiter, P., Failloux, A.B., 2022. Impact of temperature on dengue and chikungunya transmission by the mosquito *Aedes albopictus*. Sci Rep. 12 (1), 6973. https://doi.org/10.1038/s41598-022-10977-4.

Petrić, M., Ducheyne, E., Gossner, C.M., Marsboom, C., Nicolas, G., Venail, R., Hendrickx, G., Schaffner, F., 2021. Seasonality and timing of peak abundance of *Aedes albopictus* in Europe: Implications to public and animal health. Geospat Health. 16 (1), 996. https://doi.org/10.4081/gh.2021.996.

Poh, K.C., Chaves, L.F., Reyna-Nava, M., Roberts, C.M., Fredregill, C., Bueno Jr., R., Debboun, M., Hamer, G.L., 2019. The influence of weather and weather variability on mosquito abundance and infection with West Nile virus in Harris County, Texas, USA. Sci Total Environ. 675, 260–272. https://doi.org/10.1016/j.scitotenv.2019.04.109.

Prenger, J.J., Ling, P.P., 2000. Greenhouse Condensation Control. Fact Sheet (Series) AEX-800. Ohio State University Extension, Columbus, OH.

R Core Team, 2012. R: A language and environment for statistical computing. R Foundation for Statistical Computing, Vienna, Austria http://www.R-project.org/.

Rezza, G., Nicoletti, L., Angelini, R., Romi, R., Finarelli, A.C., Panning, M., Cordioli, P., Fortuna, C., Boros, S., Magurano, F., Silvi, G., Angelini, P., Dottori, M., Ciuofolini, M. G., Majori, G.C., Cassone, A., CHIKV study group, 2007. Infection with chikungunya virus in Italy: an outbreak in a temperate region. Lancet. 370, 1840–1846. https://doi.org/10.1016/S0140-6736(07)61779-6.

Roiz, D., Rosà, R., Arnoldi, D., Rizzoli, A., 2010. Effects of temperature and rainfall on the activity and dynamics of host-seeking *Aedes albopictus* females in northern Italy. Vector-Borne and Zoonotic Diseases. 10 (8), 811–816. https://doi.org/10.1089/vbz.2009.0098.

Romiti, F., Casini, R., Magliano, A., Ermenegildi, A., De Liberato, C., 2022. *Aedes albopictus* abundance and phenology along an altitudinal gradient in Lazio region (central Italy). Parasite Vector. 15, 92. https://doi.org/10.1186/s13071-022-05215-9.

Sabatini, A., Raineri, V., Trovato, G., Coluzzi, M., 1990. *Aedes albopictus* in Italia e possible diffusione della specie nell'area mediterranea. Parassitologia. 32, 30l–l.

Seager, R., Hooks, A., Williams, A.P., Cook, B., Nakamura, J., Henderson, N., 2015. Climatology, variability and trends in the U.S. vapor pressure deficit, an important fire-related meteorological quantity. J Appl Meteor Climat. 54, 1121–1141. https://doi.org/10.1175/JAMC-D-14-0321.1.

Severini, F., Toma, L., Di Luca, M., 2022. [Mosquitoes in Italy: collection, identification and conservation of the most common species]. Zanzare in Italia: raccolta, identificazione e conservazione delle specie più comuni. Roma: Istituto Superiore di Sanità. Rapporti ISTISAN 22/3.

Severini, F., Toma, L., Di Luca, M., Romi, R., 2009. Italian mosquitoes: general information and identification of adults (Diptera, Culicidae)/Le zanzare italiane: generalità e identificazione degli adulti (Diptera, Culicidae). Fragmenta Entomologica 41, 213–372. https://doi.org/10.13133/2284-4880/92.

Stojanovich, C.J., Scott, H.G., 1997. Mosquitoes of Italy: mosquitoes of the Italian biogeographic area which includes the Republic of Malta, the French Island of

Corsica and all of Italy except the Far-Northern, Provinces. Ed. Chester J, Stojanovich, Portland, Oregon (USA).

Torina, A., Sole, M., Longo, R., Romi, R., 2006. First monitoring of *Aedes albopictus* (Diptera: Culicidae) in Palermo, Sicily. Parassitologia. 48, 166.

Tran, A., L'Ambert, G., Lacour, G., Benoit, R., Demarchi, M., Cros, M., Cailly, P., Aubry-Kientz, M., Balenghien, T., Ezanno, P., 2013. A rainfall- and temperature-driven abundance model for *Aedes albopictus* populations. International Journal of Environmental Research and Public Health. 10, 1698–1719. https://doi.org/10.3390/ijerph10051698.

Walsh, A.S., Glass, G.E., Lesser, C.R., Curriero, F.C., 2008. Predicting seasonal abundance of mosquitoes based on off-season meteorological conditions. Environ Ecol Stat. 15, 279–291. https://doi.org/10.1007/s10651-007-0056-6.

Yang, B., Borgert, B.A., Alto, B.W., Boohene, C.K., Brew, J., Deutsch, K., DeValerio, J.T., Dinglasan, R.R., Dixon, D., Faella, J.M., Fisher-Grainger, S.L., Glass, G.E., Hayes Jr., R., Hoel, D.F., Horton, A., Janusauskaite, J., Kellner, B., Kraemer, M.U.G., Lucas, K.J., Medina, J., Morreale, R., Petrie, W., Reiner Jr., R.C., Riles, M.T., Salje, H., Smith, D.L., Smith, J.P., Solis, A., Stuck, J., Vasquez, C., Williams, K.F., Xue, R., Cummings, D.A.T., 2021. Modelling distribution of *Aedes aegypti* and *Aedes albopictus* using climate, host density and interspecies composition. PLoS Neglected Tropical Diseases. 15 (3), e0009063.

Zheng, X., Zhong, D., He, Y., Zhou, G., 2019. Seasonality modelling of the distribution of *Aedes albopictus* in China based on climatic and environmental suitability. Infectious Diseasees of Poverty. 8, 98. https://doi.org/10.1186/s40249-019-0612-y.

Zuur, A.F., Ieno, E.N., Elphick, C.S., 2010. A protocol for data exploration to avoid common statistical problems. Meth Ecol Evolut. 1, 3–14. https://doi.org/10.1111/j.2041-210X.2009.00001.x.